Y3.N21/5:6/1297

GOVT. DOC.

NATIONAL ADVISORY COMMITTEE FOR AERONAUTICS

TECHNICAL NOTE

No. 1297

BENDING STRESSES DUE TO TORSION IN A TAPERED BOX BEAM

By Edwin T. Kruszewski

Langley Memorial Aeronautical Laboratory
Langley Field, Va.

Washington
May 1947

CONN. STATE LIBRARY

JUN 2 1947

BUSINESS, SCIENCE & TECHNOLOGY DEPT.

NATIONAL ADVISORY COMMITTEE FOR AERONAUTICS

TECHNICAL NOTE NO. 1297

BENDING STRESSES DUE TO TORSION IN A TAPERED BOX BEAM

By Edwin T. Kruszewski

SUMMARY

A method is presented for the calculation of bending stresses due to torsion in a tapered box beam. A special taper was assumed in which all flanges, if extended, would meet at a point. The general procedure of analysis given is similar to the procedure for a nontapered beam presented by Paul Kuhn in his paper "A Method of Calculating Bending Stresses Due to Torsion," NACA ARR Dec. 1942. Recurrence formulas developed for use in this calculation are included. A comparison was made of flange and sheet stresses in boxes with varying taper, including a nontapered box.

The results obtained by this method were compared with experimental data obtained from tests performed on a tapered box beam. The box beam was tested under two independent conditions of loading: first, a concentrated torque at the tip and later, a concentrated torque at the quarter point of the span. The experimental results obtained from these tests showed good agreement with the calculated results. Calculations for the test specimen for the two loading conditions are also shown.

INTRODUCTION

The basic load-carrying structure of many aircraft wings is a box of approximately rectangular cross section consisting of the front and rear spars and the top and bottom skins of the wing. This box is stressed by both bending and torsional loads. Only the torsional loads are discussed in the present paper.

The determination of the stress distribution in a box under torsion is a relatively simple problem provided that the cross section of the box is not constrained in any manner against warping.

In this case the well-known Bredt formula for thin-walled torsion tubes is applicable. If some restraint is offered to warping, however, a set of secondary stresses is introduced in the box. Because the resultants of these secondary stresses are actually bending moments in the planes of the walls and are accompanied by the shear forces necessary to cause spanwise variation of the bending moments, these stresses are usually referred to as bending stresses due to torsion.

A method for the calculation of these bending stresses is presented in reference 1. In order to simplify the calculation, Kuhn utilizes an assumption that the cross-sectional dimensions and the torques are constant within each bay of the box and gives the solution only for boxes in which the sides are parallel. Actual wings, however, are usually tapered both in depth and in width. The present work is intended to furnish a theoretical solution of the effects of taper on bending stresses due to torsion and also to present experimental verification of the method of calculation.

The body of this paper is divided into two parts. The first part deals entirely with the theoretical development of the formulas for bending stresses due to torsion in a tapered box beam. The general procedure of analysis presented is similar to the procedures presented by Kuhn in reference 1 and by Ebner in reference 2. In order to simplify the mathematical analysis a special taper is assumed; that is, the sides of the box are assumed to taper linearly in such a way as to meet at a point.

The second part of the paper deals with the experimental verification of the theoretical formulas. A description of the test specimen and the test setup is given. Comparisons are then made of the calculated and experimental results for two independent conditions of loading. Complete numerical solutions for both loading conditions are given in the appendix.

SYMBOLS

A	effective flange area, square inches
A_F	area of flange angle, square inches
A_S	area of cover stringer, square inches

E	Young's modulus of elasticity, psi
F	flange load at any point, pounds
G	shear modulus, psi
K_1, K_2, K_3	taper constants
L	length of flange in individual bay, inches
R	taper ratio $\left(\frac{b_n}{b_{n-1}} \text{ or } \frac{c_n}{c_{n-1}}\right)$
T	external torque, inch-pounds
V	volume of material, cubic inches
X	redundant flange force, pounds
a	distance between bulkheads, inches
b	width of cover, inches
c	depth of spar, inches
f, j, p	warping constants
m	designation for general term in series
n	designation for typical bay
q	shear flow, pounds per inch
r	designation of root bay
s	distance in each bay measured along axis in flange, inches
t	sheet thickness, inches
w	warping deformation, inches
x	distance in each bay from outboard bulkhead measured along axis, inches
α_b	angle between flange and center line of cover, radians

α_c angle between flange and center line of spar, radians

σ normal flange stress, psi

τ shear stress, psi

τ_{av} average value of shear stress, psi

Subscripts:

b refers to covers

c refers to spars

i designates inboard end of bay

o designates outboard end of bay

Superscripts:

T designates stresses due to torque

U designates stresses due to dummy unit loads

X designates stresses due to X-forces

The subscripts of the redundant flange force X and of dimensions b and c designate the stations at which they exist, whereas the subscripts for T, w, p, j, and f designate the bay under consideration.

The bulkheads or stations are denoted by 0, 1, 2,... n-1, n, n+1,... r, starting from the tip or outboard end and proceeding to the root or inboard end. (See fig. 1.) The bays are also numbered from the tip, the tip bay being designated as number one (see fig. 1). A bay therefore carries the number of its inboard bulkhead or station.

DEVELOPMENT OF THEORETICAL FORMULAS

In actual wing design neither the spanwise variation of the torque nor the cross-sectional dimensions can be represented by simple mathematical expressions. In order to simplify the mathematical calculations the box is divided at the bulkheads into a number of bays and the torque is assumed constant within each individual bay.

A box beam under torsion is an indeterminate structure. In order to make the structure statically determinate, the box is cut at each bulkhead and redundant flange forces X are applied at all flanges. These X-forces are axial forces applied at each flange, as shown in figure 2. Under the action of the torque T and the flange forces X the box is deformed as shown by the dashed lines in figure 2. The amount of deformation is calculated by the use of the principle of virtual work, sometimes known as the dummy-unit-load method. The X-forces are then found by the application of the principle of consistent deformation of adjacent bays.

Sign convention.- External torques T are positive when acting clockwise as viewed from the tip. Shear stresses τ are positive when acting in the direction of shear stresses caused by positive torque. The X-forces are positive when acting in the directions shown in the sketch in figure 2. Normal stresses σ are positive when caused by positive X-forces. The warping deformation w is positive in the direction as shown by the dashed lines in figure 2.

General assumptions.- The cross section of the box is assumed to be rectangular and doubly symmetrical. The shape of the cross section is maintained by the bulkheads, which are assumed to be rigid in their own planes. In place of the actual structure, the equivalent structure shown in figure 2 is used, in which all the area capable of carrying normal stresses is concentrated in the flanges. The walls of the equivalent structure are assumed to carry only shear stresses and the flanges, all the normal stresses. In order to allow for the fact that the walls can actually carry normal stresses, each flange area is increased by one-sixth of the area of both a cover and a spar web. If the covers include stringers, an effective stringer area is added to each flange. This effective stringer area is that area which, when concentrated at the flange, gives the same section modulus about the neutral axis of the cover as the actual stringers. In the case of equally spaced stringers the effective stringer area is simply one-sixth of the total stringer area. The taper of the box is such that the flanges meet at a point. The effective flange area is assumed constant within each bay.

Stresses in an Individual Bay

The formulas given herein are derived for a typical bay n, bounded by the bulkheads n-1 and n, (fig. 2). The bay is acted on by three independent sets of loads: a torque T_n on both ends of the bay, a group of X_n-forces on the inboard end, and a group of X_{n-1}-forces on the outboard end. Formulas are derived for the stresses due to each of these independent loads. The final stress distribution may be obtained by superposing the individual stresses.

Stresses caused by torque.- The shear stresses caused by the torque acting on a bay are given by the well-known formula for shells in torsion (Bredt's formula)

$$\left.\begin{aligned} \tau_b &= \frac{T_n}{2bct_b} \\ \tau_c &= \frac{T_n}{2bct_c} \end{aligned}\right\} \qquad (1)$$

where b is the width of the cover and c the depth of the spar at some distance x from the outboard end (fig. 3). In the case of pure torque no normal stresses are set up in the flange.

Stresses caused by the X-forces.- When a set of X-forces is applied to the end of the bay, both axial stresses in the flanges and shear stresses in the walls are set up within the bay. Unlike the shear stresses for the nontapered box, the shear stresses in the tapered box are not constant throughout the bay.

In order to study the distribution of the shear stresses within the individual walls, a section of a wall is isolated as shown in figure 3(a). The free body shown in this figure is a part of a spar web bounded by two planes cutting the spar just inside the flanges and by two parallel planes, one just inside the n-1 bulkhead and another parallel to it and at a distance x from it. The

loading on the body is also shown in the figure. By summation of moments about the point of intersection of the flanges, an expression is obtained for the shear flow q_c in the spar in terms of the outboard shear flow $q_{c_{n-1}}$

$$q_c = \left(\frac{c_{n-1}}{c}\right)^2 q_{c_{n-1}} \tag{2a}$$

and, similarly, in the cover

$$q_b = \left(\frac{b_{n-1}}{b}\right)^2 q_{b_{n-1}} \tag{2b}$$

where the notation is the same as that shown in figure 3(a).

The distribution of the shear flow q_{c_x} is obtained from an infinitesimal section of a spar web isolated as shown in figure 3(b). The free body shown in this figure is a section of the spar web bounded by two parallel planes an infinitesimal distance dx apart and by two planes cutting the spar just inside the flange. From a summation of moments, the fundamental shear-flow relation in the spar for a tapered box beam is obtained,

$$q_c = q_{c_x} \tag{3a}$$

and, similarly, in the cover

$$q_b = q_{b_x} \tag{3b}$$

This equation shows that at every point along the box the shear flow acting on the flange is equal to the shear flow in the walls at that point.

In order to obtain a relationship between the shear forces in the cover and in the spars, a free body of a cross section of the

box is considered. Since the taper of the box is such that the center lines of the flanges meet at a point, the flange loads contribute no torque and the condition $\Sigma T = 0$ gives the equation,

$$q_b bc + q_c bc = 0$$

or

$$q_b = -q_c \tag{4}$$

Two expressions for the flange loads are derived, one for the X_n-forces and another for the X_{n-1}-forces. The free body of the flange in figure 3(c) shows the loading of the flange under X_n-forces only. A summation of forces along the flange shown in figure 3(c) gives an expression for the flange load F at any point along the bay:

$$F - \frac{ds}{dx}\int_0^x q_{c_x}\,dx + \frac{ds}{dx}\int_0^x q_{b_x}\,dx = 0 \tag{5}$$

where $\frac{ds}{dx}$ is a constant depending on the taper of the box. The combination of equations (2) to (5) gives

$$F = 2c_{n-1}^2\, q_{c_{n-1}} \frac{ds}{dx}\int_0^x \frac{1}{c^2}\,dx \tag{6}$$

If the integration is performed with c given as a function of x by the equation

$$c = c_{n-1}\left[1 - \left(1 - \frac{c_n}{c_{n-1}}\right)\frac{x}{a}\right] \tag{7}$$

equation (6) becomes

$$F = 2L\, q_{c_{n-1}} \frac{c_{n-1}}{c} \frac{x}{a} \tag{8}$$

where L is the length of the flange and a is the distance between bulkheads.

With the forces X_{n-1} applied at the outboard end of the bay, the flange loads become

$$F = X_{n-1} + 2L\, q_{c_{n-1}} \frac{c_{n-1}}{c} \frac{x}{a} \tag{9}$$

In order to obtain $q_{c_{n-1}}$ in terms of the X-forces, the value of F for both X_{n-1}- and X_n-forces is calculated for $x = a$. For the case of the X_n-forces

$$X_n = 2q_{c_{n-1}} \frac{c_{n-1}}{c_n} L$$

or

$$q_{c_{n-1}} = -q_{b_{n-1}} = R \frac{X_n}{2L} \tag{10}$$

For the case of the X_{n-1}-forces

$$0 = X_{n-1} + 2q_{c_{n-1}} \frac{c_{n-1}}{c_n} L$$

or

$$q_{c_{n-1}} = -q_{b_{n-1}} = -R \frac{X_{n-1}}{2L} \tag{11}$$

where R is the taper ratio = $\frac{b_n}{b_{n-1}} = \frac{c_n}{c_{n-1}}$.

By substituting equation (10) in equations (2), (4), and (8) and equation (11) in equations (2), (4), and (9), a summary of the stresses in the bay in terms of the X-forces at the end can be made. For the X_n-forces

$$\left.\begin{aligned} q_{c_x} &= \frac{c_n c_{n-1}}{c^2} \frac{X_n}{2L} \\ q_{b_x} &= -\frac{b_n b_{n-1}}{b^2} \frac{X_n}{2L} \\ \sigma &= \frac{F}{A} = \frac{c_n}{c} \frac{x}{a} \frac{X_n}{A} \end{aligned}\right\} \tag{12}$$

and for the X_{n-1}-forces

$$\left.\begin{aligned} q_{c_x} &= -\frac{c_n c_{n-1}}{c^2} \frac{X_{n-1}}{2L} \\ q_{b_x} &= \frac{b_n b_{n-1}}{b^2} \frac{X_{n-1}}{2L} \\ \sigma &= \frac{F}{A} = \left(1 - \frac{c_n}{c} \frac{x}{a}\right) \frac{X_{n-1}}{A} \end{aligned}\right\} \tag{13}$$

where A is the effective area of the flange.

Deformation of an Individual Bay

Principle of calculation.- Under the action of the torque and groups of X-forces the cross section of the box warps out of its plane, as shown in figure 2. The magnitude of this warping is calculated by the method of virtual work. The following three steps are necessary to obtain the magnitude of the warping. First, the stresses τ and σ due to the applied loads are obtained and second, the stresses τ^U and σ^U due to a system of dummy loads are calculated. These dummy loads are unit loads applied at the point where the deflections are desired and also in the direction desired. The last step is to obtain the deformation by use of the equation

$$\Sigma w = \iiint \frac{\sigma\sigma^U}{E} dV + \iiint \frac{\tau\tau^U}{G} dV \tag{14}$$

where V is the volume of the stressed material. This equation is based on the principle that the external work done by the unit force must equal the internal energy stored by virtue of the existence of the unit force.

Examination of figure 2 shows that the warping is doubly antisymmetrical and consequently the dummy loads employed in the solution are also doubly antisymmetrical. This group of unit loads is similar to the group of X-forces and therefore the formulas for the X-forces can be used in the calculation of the stresses caused by dummy loads.

Warping caused by torque.- The stresses caused by the torque acting on the box are, from formula (1),

$$\left.\begin{aligned} \sigma &= 0 \\ \tau_b &= \frac{T_n}{2bct_b} \\ \tau_c &= \frac{T_n}{2bct_c} \end{aligned}\right\} \tag{15}$$

In order to obtain the warping in the nth bay at bulkhead n, the antisymmetrical group of unit loads is applied at the inboard end of the bay. The stresses caused by these forces are calculated from formulas (12) by placing $X_n = -1$. The results are

$$\left.\begin{aligned} \sigma^U &= -\frac{c_n}{c}\frac{x}{a}\frac{1}{A} \\ \tau_c^U &= -\frac{c_n c_{n-1}}{c^2}\frac{1}{2Lt_c} \\ \tau_b^U &= \frac{b_n b_{n-1}}{b^2}\frac{1}{2Lt_b} \end{aligned}\right\} \qquad (16)$$

The results for σ, τ_b, and τ_c and for σ^U, τ_b^U, and τ_c^U given in equations (15) and (16) are now substituted in equation (14) to give

$$4w_{n_i}^T = 2\int_0^{a_c}\frac{1}{G}\frac{T_n}{2bct_c}\left(-\frac{c_n c_{n-1}}{c^2}\frac{1}{2Lt_c}\right)ct_c\,dx_c + 2\int_0^{a_b}\frac{1}{G}\frac{T_n}{2bct_b}\left(\frac{b_n b_{n-1}}{b^2}\frac{1}{2Lt_b}\right)bt_b\,dx_b$$

which yields when integrated

$$w_{n_i}^T = \frac{T_n}{8Gb_{n-1}c_{n-1}}\left(\frac{a_b}{L}\frac{b_{n-1}}{t_b} - \frac{a_c}{L}\frac{c_{n-1}}{t_c}\right)\frac{1+R}{2R} \qquad (17)$$

In order to obtain the warping due to torsion at bulkhead n-1, the groups of unit loads are applied at the outboard end of the bay. Now the stresses due to the dummy loads are calculated from formula (13) with $X_{n-1} = 1$. The results are as follows:

$$\left.\begin{aligned} \sigma^U &= \frac{1}{A}\left(1 - \frac{c_n}{c}\frac{x}{a}\right) \\ \tau_c^U &= -\frac{c_n c_{n-1}}{c^2}\frac{1}{2Lt_c} \\ \tau_b^U &= \frac{b_n b_{n-1}}{b^2}\frac{1}{2Lt_b} \end{aligned}\right\} \tag{18}$$

The stresses due to the torque acting on the bay are those shown in equation (15). An inspection of the stresses (equations (16) and (18)) caused by the unit loads gives

$$w_{n_o}^T = w_{n_i}^T = w_n^T \tag{19}$$

Warping caused by X_n-forces.- The warping at the inboard end of the bay caused by the X_n-forces is obtained by the application of equation (14) in the form

$$4w_{n_i}^{X_n} = 4\int_0^L \frac{\sigma\sigma^U}{E} A\,ds + 2\int_0^{a_b} \frac{\tau_b \tau_b^U}{G} bt_b\,dx_b + 2\int_0^{a_c} \frac{\tau_c \tau_c^U}{G} ct_c\,dx_c \tag{20}$$

Substitution of the values for the stresses due to the unit loads (equation (16)) and the stresses due to the X_n-forces (equation (12)) in equation (20), causes the equation for warping to become

$$w_{n_i}^{X_n} = -p_n X_n \tag{21}$$

where

$$p_n = K_1 \frac{L}{3EA} + \frac{1}{8GL}\left(\frac{a_b}{L}\frac{b_{n-1}}{t_b} + \frac{a_c}{L}\frac{c_{n-1}}{t_c}\right)\frac{1+R}{2} \qquad (22)$$

and

$$K_1 = \frac{3R^2}{(R-1)^3}\left(\frac{R^2-1}{R} - 2\log_e R\right) \qquad (23)$$

The constant K_1 is dependent entirely on the taper ratio for the individual bays.

As the value of the taper ratio approaches unity, the expression for K_1 in equation (23) becomes too sensitive for practical use. By expanding the logarithm into an infinite series of $(R - 1)$,

$$K_1 = 1 + \frac{1}{2}(R-1) - \frac{1}{5}(R-1)^2 + \frac{1}{10}(R-1)^3 \ldots$$

$$+ (-1)^{m+1}\frac{12}{(m+1)(m+2)(m+3)}(R-1)^m \qquad (24)$$

This expression can only be used for small values of R, since the series converges only for values of $R < 2$. The rate of convergence is very slow, however, after R reaches a value of approximately 1.5. For values of $R < 1.5$ only four terms of the series are needed to evaluate K_1 within 1 percent. A graph of numerical values for K_1 from $R = 1.00$ to $R = 3.00$ can be seen in figure 4.

The warping at the outboard end of the bay caused by the X_n-forces can be written in the form

$$w_{n_o}^{X_n} = -j_n X_n \qquad (25)$$

where the coefficient j_n is obtained by the application of equation (14). By substituting the values for unit stresses from equation (18) and the value for X_n-stresses from equation (12) into equation (14) and integrating the result, j_n is found to be given by

$$j_n = -K_2 \frac{L}{6AE} + \frac{1}{8GL}\left(\frac{a_b}{L}\frac{b_{n-1}}{t_b} + \frac{a_c}{L}\frac{c_{n-1}}{t_c}\right)\frac{R+1}{2} \tag{26}$$

where

$$K_2 = -6\left[\frac{2R^2 - 2R - (1+R)\,R \log_e R}{(R-1)^3}\right] \tag{27}$$

For small values of R, again the expanded series for K_2,

$$K_2 = 1 - \frac{1}{10}(R-1)^2 + \frac{1}{10}(R-1)^3 \ldots + (-1)^{m+1}\frac{6(m-1)}{(m+1)(m+2)(m+3)}(R-1)^m \tag{28}$$

is more practical. As for K_1, the rate of convergence of the series makes the expression practical only for the range from R = 1.00 to R = 1.50. The numerical values for K_2 are plotted in figure 4.

Warping caused by X_{n-1}-forces.- The warping at the inboard end of the bay, caused by the X_{n-1}-forces, can be shown, by means of Maxwell's law of reciprocal deflection, to be equal to

$$w_{n_i}^{X_{n-1}} = j_n X_{n-1} \tag{29}$$

where j_n is the expression given in equation (26).

The warping at the outboard end of the bay is derived by substituting the values of the stresses for unit loads from equation (18) and the values of the stresses for the X_{n-1}-forces from equation (13) into equation (14). Upon integrating the result, the following expression is obtained:

$$w_{n_o}^{X_{n-1}} = f_n X_{n-1} \tag{30}$$

where

$$f_n = K_3 \frac{L}{3EA} + \frac{1}{8G_L} \left(\frac{a_b}{L} \frac{b_{n-1}}{t_b} + \frac{a_c}{L} \frac{c_{n-1}}{t_c} \right) \frac{1 + R}{2} \tag{31}$$

and

$$K_3 = 3 \left[\frac{(R^2 - 1) - 2R \log_e R}{(R - 1)^3} \right] \tag{32}$$

For small values of R, the expanded series form for K_3,

$$K_3 = 1 - \frac{1}{2}(R - 1) + \frac{3}{10}(R - 1)^2 - \frac{1}{5}(R - 1)^3 \ldots$$

$$+(-1)^m \frac{6}{(m + 2)(m + 3)} (R - 1)^m \tag{33}$$

should be used. As was the case for the expressions for K_1 and K_2, the rate of convergence of the series makes the expression for K_3 practical only within the limits of $R = 1.00$ and $R = 1.50$.

Comparison of tapered-box formulas with uniform cross-section formulas.- A comparison of the formulas derived for the tapered box beams with those formulas derived for the nontapered box by Kuhn in reference 1 can easily be made by obtaining the formulas for the special case of taper where the taper ratio is unity.

With this assumption, the following relations hold true

$$a = a_b = a_c = L$$

$$K_1 = K_2 = K_3 = 1$$

Equation (17) now becomes

$$w_n^T = \frac{T}{8Gbc}\left(\frac{b}{t_b} - \frac{c}{t_c}\right)$$

which is identical with equation (21) of reference 1. Equations (22) and (31) become

$$p_n = f_n = \frac{a}{3EA} + \frac{1}{8Ga}\left(\frac{b}{t_b} + \frac{c}{t_c}\right)$$

which is identical with equation (23) of reference 1. Equation (26) becomes

$$j_n = -\frac{a}{6AE} + \frac{1}{8Ga}\left(\frac{b}{t_b} + \frac{c}{t_c}\right)$$

which is identical with equations (27) of reference 1.

This comparison shows that all the tapered-box formulas for the special case of $R = 1.0$ or uniform cross section are identical with those formulas developed in reference 1.

Derivation of a recurrence formula.- The total warping at the ends of the bay n due to the combined effects of the three separate forces T, X_n, and X_{n-1} can now be obtained by a summation of all the component parts. The equation for the warping at the inboard end of bay n is given by the sum of equations (19), (21), and (29)

$$w_{n_i} = w_n^T - p_n X_n + j_n X_{n-1} \qquad (34)$$

The equation for warping at the outboard end of bay n given by the summation of equations (19), (25), and (30) is

$$w_{n_o} = w_n^T - j_n X_n + f_n X_{n-1} \tag{35}$$

The equation for warping at the outboard end of bay n + 1 is obtained merely by increasing all subscripts of equation (35) by one and is

$$w_{(n+1)_o} = w_{n+1}^T - j_{n+1} X_{n+1} + f_{n+1} X_n \tag{36}$$

According to the principle of consistent deformation, the warping at the outboard end of one bay must be equal to the warping at the inboard end of the adjacent bay. A recurrence formula can therefore be obtained by equating the warping formulas of two adjacent bays. By equating the expression for w_{n_i} in equation (34) and the expression for $w_{(n+1)_o}$ in equation (36), the general recurrence formula becomes

$$j_n X_{n-1} - \left(f_{n+1} + p_n \right) X_n + j_{n+1} X_{n+1} = w_{n+1}^T - w_n^T \tag{37}$$

By giving n successive values from n = 1 to n = r, a set of r equations is obtained, each of which contains three of the redundant X-forces. These equations represent the continuity conditions at stations 1 to r. The tip of the box is usually free from any restraint, thereby making the force X_o at the tip of the box zero. Therefore, for a box divided into r bays, r redundant forces and r equations exist.

Boundary condition.- With the tip of the box free from any restraints and the tip force $X_o = 0$, the first equation of the system is

$$-\left(f_2 + p_1 \right) X_1 + j_2 X_2 = w_2^T - w_1^T \tag{38}$$

When a beam is attached to a rigid foundation, the foundation may be considered a bay $r + 1$ having infinite shear stiffness and infinite axial stiffness; therefore,

$$w_{r+1} = f_{r+1} = J_{r+1} = 0$$

The last equation of the system now becomes

$$J_r X_{r-1} - P_r Y_r = -w_r^T \tag{39}$$

Comparison of stresses for boxes with varying taper ratio and flange area.- In order to show the effect of taper on the bending stresses due to torsion, calculations were made of the flange and sheet stresses for boxes with varying taper ratio and flange area. All boxes were 120 inches long and were divided into six bays of equal length. The root sections of the boxes were identical. The dimensions for the boxes at the root and tip can be seen in table 1.

In figure 5(a), curves of the flange stresses are drawn for the three boxes with constant flange areas and also for the moderately and highly tapered boxes with a tapered flange area. In figure 5(b), curves of the sheet stresses are drawn only for the three boxes with the tapered flange area.

Figure 5(a) shows that the flange stresses for the case of the moderately tapered box (curves C and D) are only slightly greater than those of the nontapered box (curve E). Examination of the root flange stresses for all cases shows that the increase in these stresses for an increase in taper is very small; the root flange stress for the highly tapered box is approximately 10 percent above that of the nontapered box. Since, as in the nontapered box, the flange stresses for the box with moderate taper decrease very rapidly, the only appreciable flange stresses occur in the vicinity of the root. As the taper becomes greater, however, the flange stresses along the total span increase. Inspection of curves A and B shows that the flange stresses at a point 20 inches from the tip are approximately one-third of the maximum flange stresses at the root. Consequently, for the box beam with moderate taper the bending stresses due to torsion in the outboard end are negligible as compared with the stresses near the root, whereas in the highly tapered box the flange stresses do become appreciable. A similar conclusion for the sheet stresses can be reached by the inspection of figure 5(b).

Comparison of curves A and B and curves C and D in figure 5(a) shows the effect of a variation of flange area along the span on the flange stresses. The maximum effect appears near the tip of the box where the flange stress for the box with tapered-flange areas is approximately 20 percent higher than the flange stress in the box with constant flange area.

Two sets of calculations for the root stresses were made for a moderately tapered box under a distributed torque loading. The distribution of the torque was such that the increment of torque in each bay was proportional to the chord of the bay at the inboard end. The method presented herein is used for the first calculation which was an exact solution of the root stresses. The second calculation was made on the assumption that the box consisted only of the root bay with the total torque acting on the outboard end. The result of these calculations showed that the root stresses calculated by means of the exact method were approximately 10 percent greater than the root stresses calculated by the approximate method. Similar results were observed for a calculation of the stresses in the highly tapered box under a similar distribution of torque. When only the approximate value of the stresses at the root is required, a satisfactory answer can be obtained by assuming that the box consists only of the root bay and that the total torque is concentrated at the outboard end of that bay.

In both sets of calculations with the distributed torque, the flange stresses near the tip of all the boxes were approximately of the same order of magnitude as those of the moderately tapered box with tip loading shown in figure 5(a).

EXPERIMENTAL VERIFICATION OF FORMULAS

Test specimens.- In order to obtain experimental verification of the formulas derived herein, a large tapered box beam was constructed and tested. The box was made symmetrical about the midspan and was supported there by a rigid frame as shown in figure 6. Because of this setup, complete restraint against warping at the root, which is the midspan of the box, was assured. Equal torques were applied at the tips and later at the quarter points of the span.

The material used for the box was 24S-T aluminum alloy and the general dimensions of the specimen are shown in figure 7. The thicknesses of the covers and the spar webs and the sizes of the flanges, stiffeners, and stringers are also shown in figure 7. General dimensions and stringer spacing of both the root and

tip sections are shown in figure 8, along with the dimensions for the equivalent substitute sections. The dimensions of the box vary linearly from the tip to the root, whereas the thicknesses of the sheets and sizes of the flanges and stringers are constant for the whole box. Although the flange area of the simplified structure varies linearly from the tip to the root, due to the addition of one-sixth the area of the cover and spar web, an average flange area in each bay is used in the calculations. In order to assure that the bulkheads were rigid for all practical purposes, the bulkheads were made of formed $\frac{1}{8}$-inch steel plate.

Test setup.- The general test setup is shown in figure 6. The box beam was connected to the center tower by means of four steel flexure plates, one on each side of the box. In order to reduce the end effects as much as possible, the box was connected to the flexure plates at the root by closely spaced $\frac{1}{4}$-inch bolts. This type of connection permits the torque reaction to be distributed as a uniform shear flow around the perimeter of the box. Figure 6 shows the loading arrangment at the tips of the box. The same method of loading was used when the tests were run with loads at the quarter-span points.

Test procedure.- Strain surveys were made for both loadings with 2-inch Tuckerman optical strain gages. Shear-strain measurements were taken around the perimeter of the box at sections near the center line of each bay, and also at sections $1\frac{1}{2}$ inches on either side of bulkheads 4 and 5. The shear-strain measurements across any cross section consisted in measurements made between the stringers and between the flange and adjacent stringer on the covers and three equally spaced measurements in the spar web. The shear stresses were obtained from strain readings at 45° and 135° from the axis of the structure. The normal strains were measured along each flange at approximately 3-inch intervals starting at $4\frac{1}{2}$ inches from the root.

For each test run, strain-gage readings were taken at zero torque and after each of four equal increments of 75,000 inch-pounds of torque. The load was then released and another zero reading was taken. If the two sets of zero readings did not agree within 100 psi, a new test run was made. The strain readings for each gage were then plotted against torque and the best straight line was drawn through the points. If the line did not intersect the origin, a parallel line was drawn through the origin. If, however, the new line was displaced

from the original line by more than a strain equivalent to 200 psi, a new set of readings was taken. The values of strain were then obtained from this new parallel line.

Test results.- In converting the results obtained from the strain surveys to stresses, Young's modulus was taken as 10,600 ksi and the shear modulus as 4,000 ksi.

The observed shear stress of a cover or a spar at any section is the average of the shear stresses obtained for the two opposite covers or spars at that section. Figure 9 shows that the distribution of the shear stresses across the covers and spars is constant throughout the section, except for the part of the skin between the flange and the adjacent stringer. These plots substantiate in part the original assumption of uniform shear stresses over the cross section.

The observed flange stress at any section is the average of the flange stresses obtained for the four flanges at that section. In figure 10 a plot of the stringer stresses at a cross section in bays 5 and 6 is shown. Strain readings were taken on each stringer on the leg adjacent to the cover. The cross section in bays 5 and 6 were chosen because the normal stresses were the largest in those bays. Figure 10 shows that the chordwise distribution of the stringer stresses in the cover is approximately linear; thereby the use of the theoretical equivalent-area coefficient of one-sixth appears to be justified.

Comparison of test results with theoretical curves.- A comparison of the observed and calculated shear flow and normal flange stresses for both loading conditions can be seen in figures 11 to 14. The stresses were calculated as shown in the appendix by means of the formulas presented in this paper.

Examination of figures 11 and 12 shows very good agreement between the observed and calculated shear-stress values. The only point in the tip loading condition (fig. 11) that does not fall on the calculated curve within the accuracy of the Tuckerman gage readings is a point on the spar 7.5 inches from the tip, which is approximately 5 percent greater than the corresponding calculated value. This deviation from the calculated curve is probably caused by the fact that the section at which this measurement is taken is near the tip of the box where the load is being applied.

Examination of figures 13 and 14 shows good agreement between the experimental and calculated values of the axial loads in the flange due to torsion. For both loading conditions, the observed

values in bays 5 and 6, which include the most critical loads (the loads at the root of the box), agree within the accuracy of the Tuckerman gage reading. The observed values in bays 3 and 4 compare favorably with the calculated values for the tip-loading condition. For the quarter-point loading condition, however, the observed values for the test points in the vicinity of bulkhead 3 are slightly greater than the calculated values for the same points. This deviation from the calculated values can be explained by the uncertainty of the conditions at the point of loading. The extent to which the loading fixture restrains the flanges from warping and the fact that the torque applied to the box through the spar webs needs an appreciable distance to be distributed are only the obvious reasons for deviations to occur in the vicinity of the loading bulkheads. Also for these reasons, no attempt was made to evaluate the stresses in the tip bay for the tip loading condition.

The values of the experimental stresses in figures 13 and 14, taken within 5 inches of bulkheads 1 and 2, are somewhat greater than the calculated values. This deviation may be explained in part by local bending of the flange. The flange acts as a continuous beam supported by an elastic foundation and loaded at each bulkhead. The bending moment in this beam is the greatest at the bulkheads where the deviation of the observed values from the calculated values are the greatest.

CONCLUDING REMARKS

The agreement that was obtained between the experimental bending stresses due to torsion in a tapered box beam and the calculated values indicates that the method presented can be used to obtain the bending-stress distribution in a tapered box beam under torsion.

For boxes with very small taper the flange stresses in the outboard half of the box are very small. In these boxes a first approximation of the bending stresses due to torsion can be made by using the properties of the tapered box at the root, by considering the box nontapered, and then using the method of

analysis described by Paul Kuhn in his paper on bending stresses due to torsion (NACA ARR, Dec. 1942). For more accurate calculations of the bending stresses due to torsion in a tapered box, however, the method presented herein should be used.

Langley Memorial Aeronautical Laboratory
National Advisory Committee for Aeronautics
Langley Field, Va., February 13, 1947

APPENDIX

SOLUTION OF STRESS DISTRIBUTION IN TAPERED BOX BEAM

In order to give an illustration of the method, a complete solution of the shear and normal stress distribution in the tapered box used as a test specimen is given.

The actual over-all dimensions of the specimen are given in figure 7. The dimensions at the root and tip cross sections are given in figure 8, together with the dimensions for the equivalent structure. The effective flange area is obtained from the equation

$$A = A_F + \frac{1}{6}\Sigma A_S + \frac{1}{6}bt_b + \frac{1}{6}ct_c \qquad (A1)$$

where A_F is the area of a flange angle and A_S is the area of a cover stringer. The effective flange areas are assumed to be concentrated at the points of intersection of the center lines of the cover sheets and spar webs. All properties of the equivalent box taper linearly from tip to root. The box is divided into six bays. The geometrical properties for the inboard and outboard end of each bay are listed in table 2.

The values of E and G used in these calculations are, respectively, 10,600 ksi and 4,000 ksi. For the first loading condition, a torque of 100,000 inch-pounds is applied to the tip of the box and for the second loading condition a torque of 100,000 inch-pounds is applied to the middle bulkhead of the box.

The warping constants p, j, and f, calculated by means of the equations (22), (26), and (31), and the warping due to

torsion w_n^T, calculated by the use of equation (17), are tabulated in the following table. The tabulated w_n^T values are for the load at tip of box.

Bay	Warping constants			
	p_n	j_n	f_n	w_n^T
1	1.610×10^{-6}	0.829×10^{-6}	1.564×10^{-6}	6439×10^{-6}
2	1.581	.574	1.511	5848
3	1.647	.684	1.585	5274
4	1.714	.794	1.660	4803
5	1.785	.904	1.739	4410
6	1.857	1.011	1.817	4083

For a box with six bays, the recurrence formula (equation (37)) and the equations for the boundary conditions (equations (38) and (39)) give the following six equations.

$$\left.\begin{aligned}
-(p_1 + f_2)X_1 + j_2X_2 &= w_2^T - w_1^T \\
j_2X_1 - (p_2 + f_3)X_2 + j_3X_3 &= w_3^T - w_2^T \\
j_3X_2 - (p_3 + f_4)X_3 + j_4X_4 &= w_4^T - w_3^T \\
j_4X_3 - (p_4 + f_5)X_4 + j_5X_5 &= w_5^T - w_4^T \\
j_5X_4 - (p_5 + f_6)X_5 + j_6X_6 &= w_6^T - w_5^T \\
j_6X_5 - p_6X_6 &= -w_6^T
\end{aligned}\right\} \quad (A2)$$

From substitution of the values from the preceding table into the formulas of equation (A2), the following set of simultaneous equations is obtained for the first tip loading condition:

X_1	X_2	X_3	X_4	X_5	X_6	$w_{n+1} - w_n$
-3.121	0.574					-591
.574	-3.166	0.684				-574
	.684	-3.307	0.794			-471
		.794	-3.453	0.904		-393
			.904	-3.602	1.011	-327
				1.011	-1.857	-4083

The solution of these equations gives

$$X_1 = 244 \qquad X_4 = 437$$
$$X_2 = 292 \qquad X_5 = 965$$
$$X_3 = 307 \qquad X_6 = 2724$$

These values give the flange loads at each bulkhead. In order to obtain the distribution of the flange loads between the bulkheads, the formula

$$F = X_{n-1} + \left(X_n - X_{n-1}\right) \frac{c_n}{c} \frac{x}{a} \tag{A3}$$

obtained from a summation of equations (12) and (13) is used.

For calculation of the distribution of the shear flow along the span of the box, the formulas

$$q_{c_x} = \frac{c_n c_{n-1}}{c^2} \frac{1}{2L} \left(X_n - X_{n-1}\right) + \frac{T}{2bc}$$

and

$$q_{b_x} = -\frac{c_n c_{n-1}}{c^2} \frac{1}{2L} \left(X_n - X_{n-1}\right) + \frac{T}{2bc} \tag{A4}$$

obtained from a summation of equations (1), (12), and (13) are used. A tabulation of the flange loads and shear flows can be seen in table 3.

For the quarter-point loading condition the values for the warping constants p, j, and f are the same as those for the tip loading condition. Also the values for w_n^T are the same except in bays 1, 2, and 3 where w_n^T is zero. The formulas (A2) can still be used for this loading condition. By substituting the appropriate values in equation (A2), the following set of simultaneous equations is obtained for the quarter-point loading condition:

X_1	X_2	X_3	X_4	X_5	X_6	$w_{n+1} - w_n$
-3.121	0.574					0
.574	-3.166	0.684				0
	.684	-3.307	0.794			4803
		.794	-3.453	0.904		-393
			.904	-3.602	1.011	-327
				1.011	-1.857	-4083

The solution of these equations gives

$X_1 = -63$ $\quad X_4 = -21$

$X_2 = -343$ $\quad X_5 = 829$

$X_3 = -1528$ $\quad X_6 = 2650$

Again, by the use of the equations (A3) and (A4) the distribution of the flange loads and shear flows was obtained along the span. The tabulations of these flange loads and shear flows are shown in table 4.

REFERENCES

1. Kuhn, Paul: A Method of Calculating Bending Stresses Due to Torsion. NACA ARR, Dec. 1942.

2. Ebner, Hans: Torsional Stresses in Box Beams with Cross Sections Partially Restrained against Warping. NACA TM No. 744, 1934.

TABLE 1

ROOT AND TIP DIMENSIONS OF BOX BEAMS

Section	b (in.)	c (in.)	t_b (in.)	t_c (in.)	A (Constant) (sq in.)	A (Tapered) (sq in.)
Root	50.000	10.000	0.064	0.072	1.000	1.000
Tip:						
Highly tapered	20.000	4.000	.064	.072	1.000	.200
Moderately tapered	35.000	7.000	.064	.072	1.000	.200
Nontapered	50.000	10.000	.064	.072	1.000	.200

NATIONAL ADVISORY
COMMITTEE FOR AERONAUTICS

TABLE 2

GEOMETRICAL PROPERTIES OF BAYS IN TAPERED BOX BEAM

Bay	a (in.)	a_c (in.)	a_b (in.)	L (in.)	c_{n-1} (in.)	c_n (in.)	b_{n-1} (in.)	b_n (in.)	t_c (in.)	t_b (in.)	A (sq in.) (a)	R	K_1	K_2	K_3
1	15.0	15.050	15.000	15.050	5.869	6.416	26.132	28.602	0.0700	0.0629	0.935	1.093	1.045	0.998	0.955
2	20.0	20.067	20.003	20.071	6.416	7.146	28.602	31.896	.0700	.0629	.972	1.114	1.054	.997	.946
3	20.0	20.067	20.003	20.071	7.146	7.875	31.896	35.190	.0700	.0629	1.015	1.102	1.050	.998	.950
4	20.0	20.067	20.003	20.071	7.875	8.605	35.190	38.484	.0700	.0629	1.059	1.093	1.045	.998	.955
5	20.0	20.067	20.003	20.071	8.605	9.334	38.484	41.778	.0700	.0629	1.101	1.085	1.040	.998	.960
6	20.0	20.067	20.003	20.071	9.334	10.064	41.778	45.072	.0700	.0629	1.145	1.078	1.037	.999	.963

[a]Average of effective areas at inboard and outboard ends of bay.

NATIONAL ADVISORY
COMMITTEE FOR AERONAUTICS

TABLE 3

CALCULATED NORMAL AND SHEAR STRESSES IN TAPERED BOX BEAM FOR LOAD AT TIP

[T = 100,000 in.-lb]

Bay	Distance from tip (in.)	F (lb)	σ (psi)	q_c (lb/in.)	τ_c (psi)	q_b (lb/in.)	τ_b (psi)
1	0	0	0	334.9	4780	317.1	5040
	10	167	178	296.7	4240	280.9	4470
	15	244	257	279.9	4000	265.1	4210
2	15	244	257	273.8	3910	271.2	4310
	25	269	277	245.0	3500	242.6	3860
	35	292	294	220.4	3150	218.2	3470
3	35	292	294	219.7	3140	218.9	3480
	45	300	296	198.9	2840	198.1	3150
	55	307	296	180.7	2580	180.1	2860
4	55	307	296	183.9	2630	176.9	2810
	65	375	354	167.9	2400	161.5	2570
	75	437	405	154.0	2200	148.0	2350
5	75	437	405	165.3	2360	136.7	2170
	85	712	647	152.0	2170	125.8	2000
	95	965	859	140.3	2000	116.1	1850
6	95	965	859	175.3	2500	81.1	1290
	105	1878	1640	162.3	2320	75.1	1190
	115	2724	2336	150.8	2150	69.6	1110

TABLE 4

CALCULATED NORMAL AND SHEAR STRESSES IN TAPERED BOX BEAM FOR LOAD AT QUARTER POINT OF SPAN

Bay	Distance from tip (in.)	F (lb)	σ (psi)	q_c (lb/in.)	τ_c (psi)	q_b (lb/in.)	τ_b (psi)
T = 0							
	0	0	0	-2.3	-30	2.3	40
1	10	-43	-46	-2.0	-30	2.0	30
	15	-63	-66	-1.9	-30	1.9	30
	15	-63	-66	-7.8	-110	7.8	120
2	25	-211	-217	-6.9	-100	6.9	110
	35	-343	-345	-6.3	-90	6.3	100
	35	-343	-345	-32.5	-460	32.5	520
3	45	-965	-951	-29.4	-420	29.4	470
	55	-1528	-1473	-26.8	-380	26.8	430
T = 100,000 in.-lb							
	55	-1528	-1473	221.5	3160	139.3	2210
4	65	-740	-699	202.1	2890	127.3	2020
	75	-21	-19	185.4	2650	116.6	1850
	75	-21	-19	174.0	2490	128.0	2030
5	85	421	382	160.0	2290	117.8	1870
	95	829	738	147.8	2110	108.6	1730
	95	829	738	177.0	2530	79.4	1260
6	105	1774	1549	163.9	2340	73.5	1170
	115	2650	2273	152.3	2180	68.1	1080

Figure 1.— Convention for numbering bays and bulkheads.

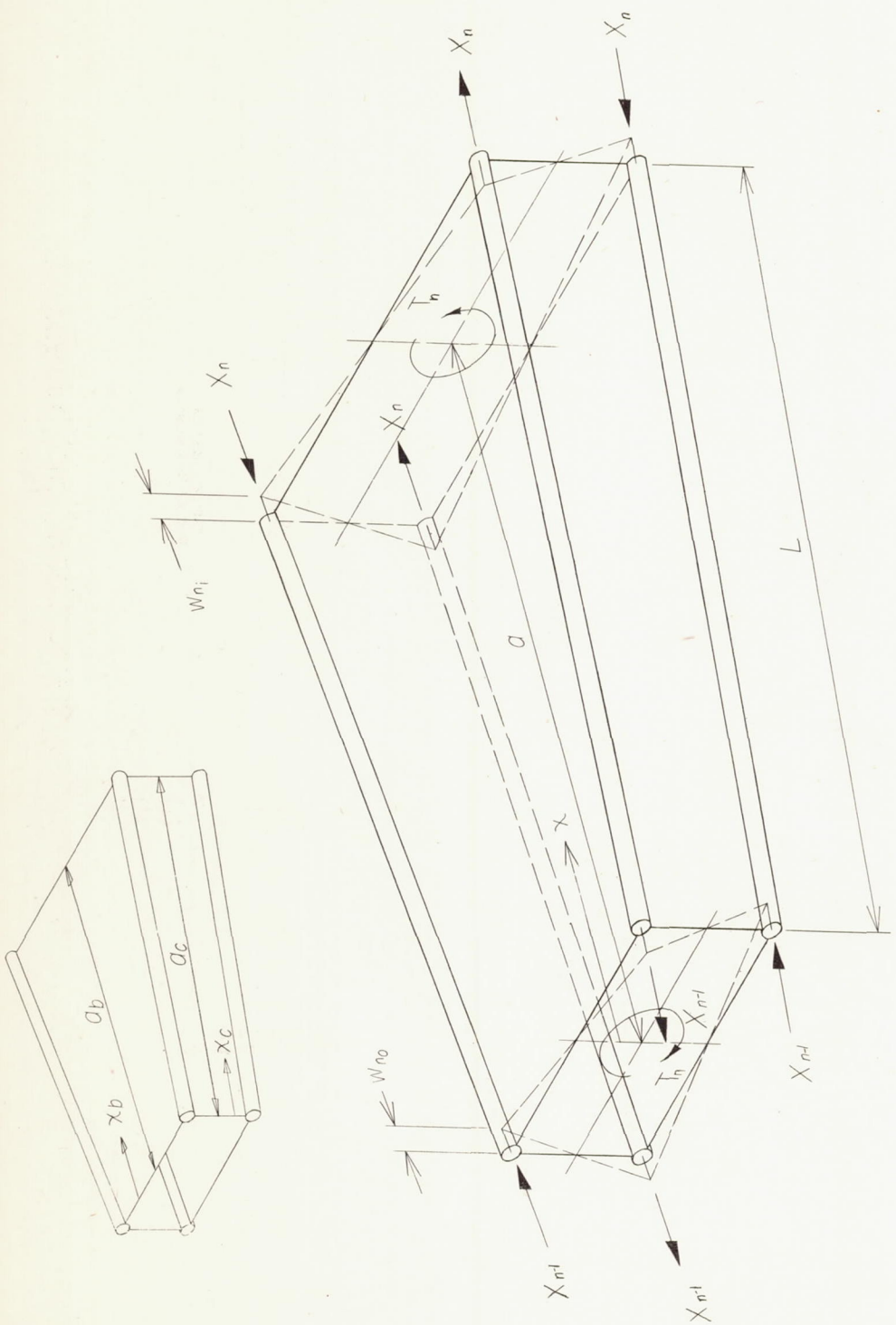

Figure 2.—Free-body sketch of typical bay n.

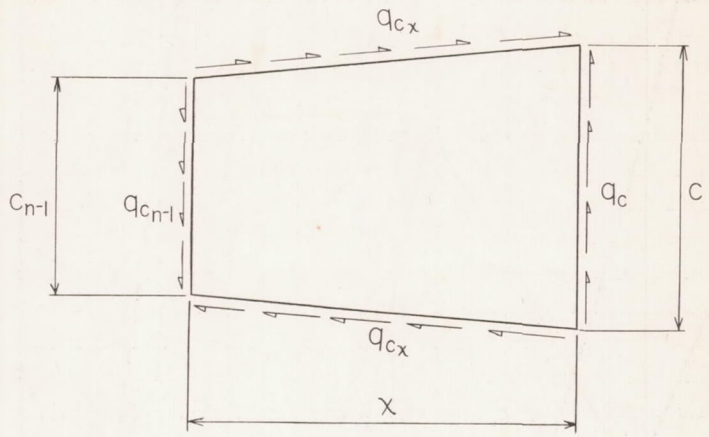

(a) Free-body sketch of section of spar web.

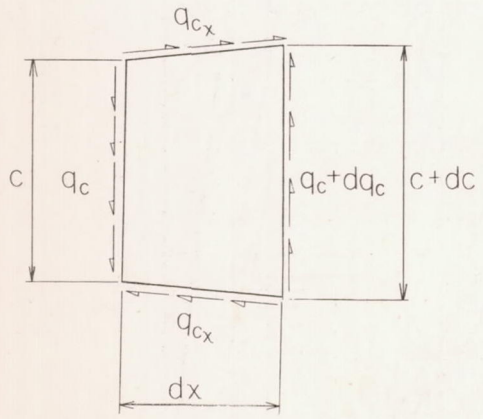

(b) Infinitesimal section of spar web.

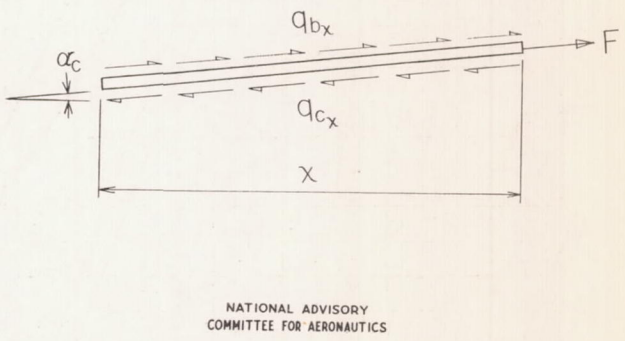

(c) Free-body sketch of flange.

Figure 3.—Free-body sketches of component parts of spar.

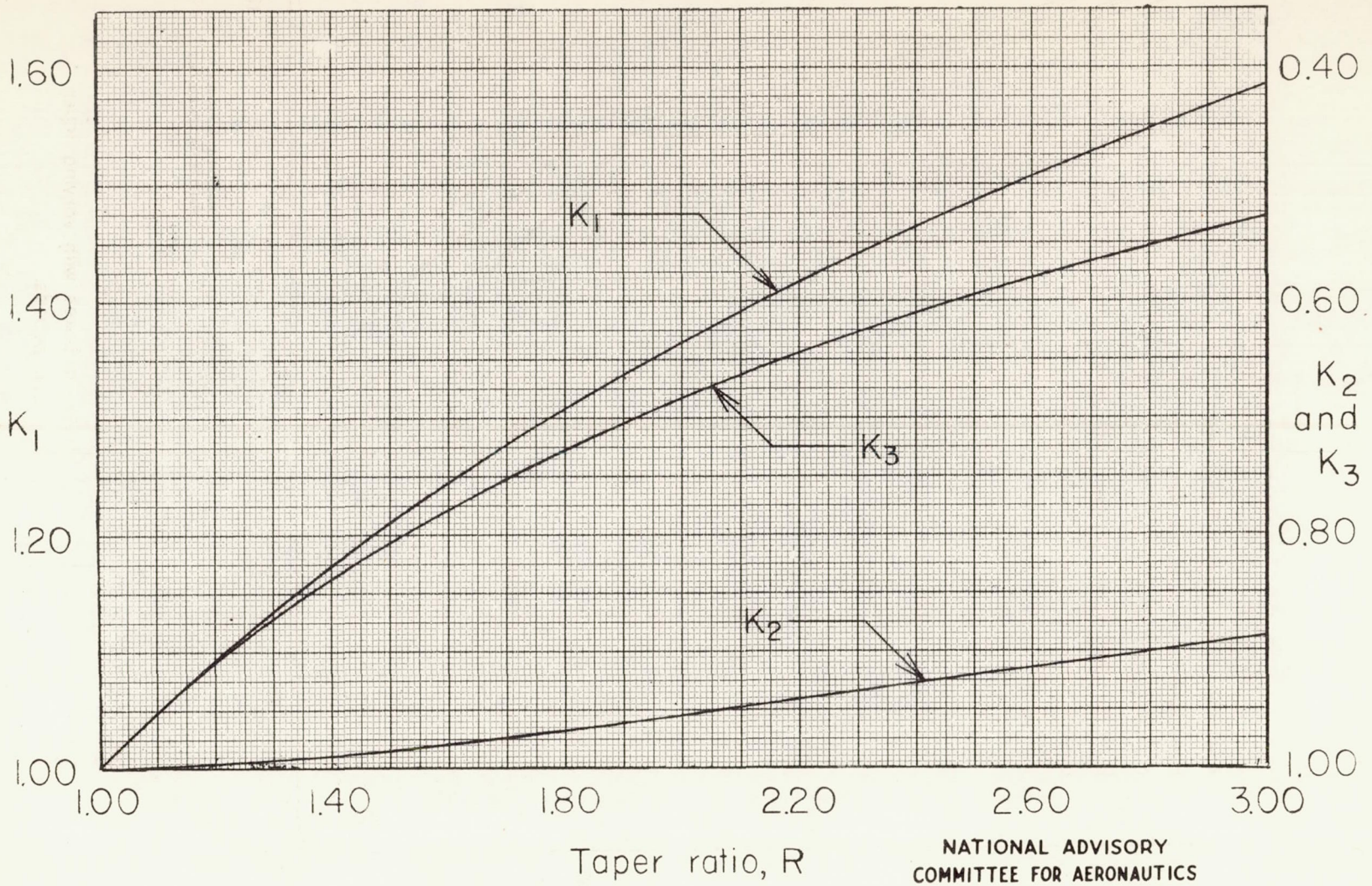

Figure 4.—Variation of taper constants with taper ratio.

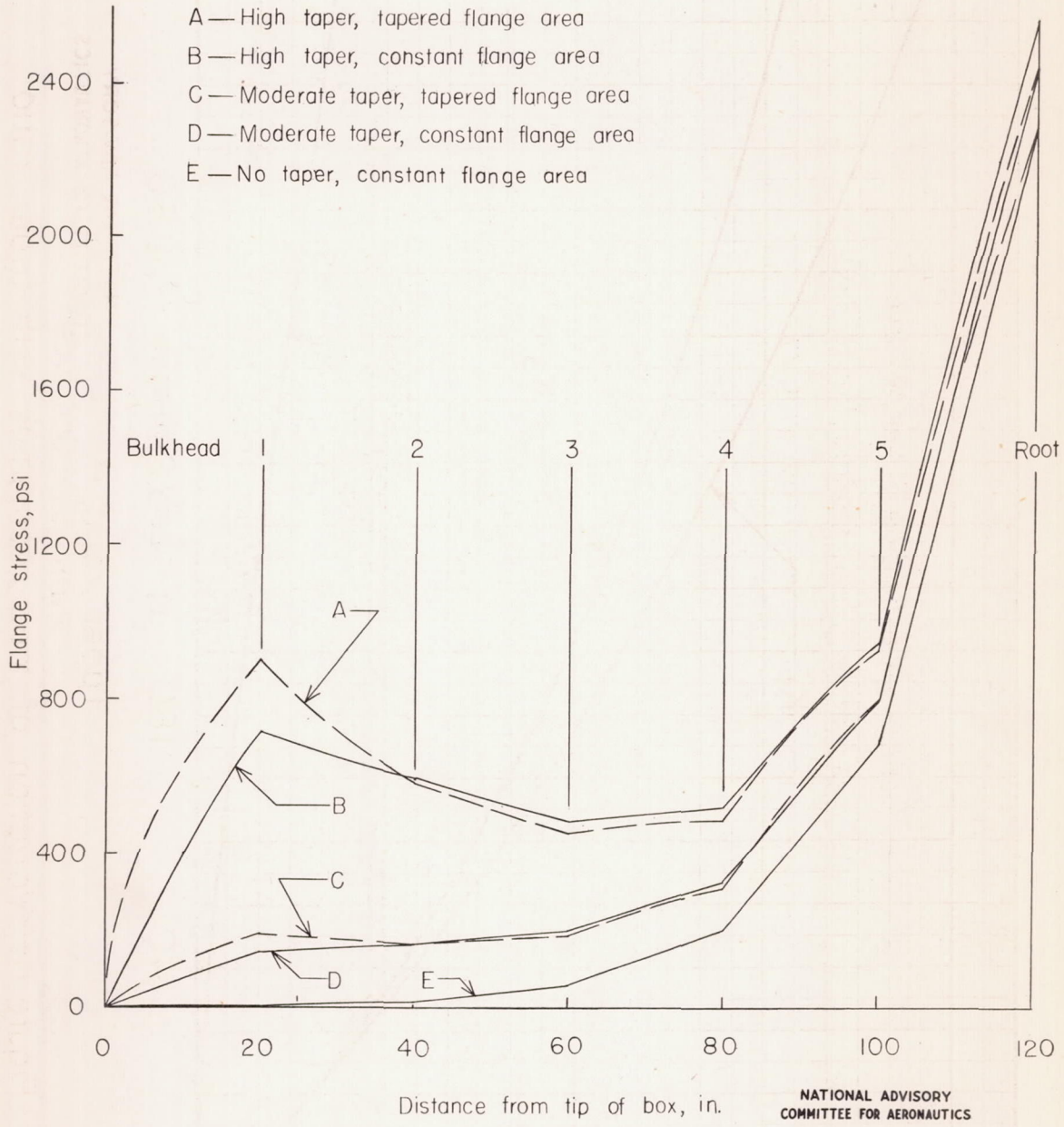

(a) Flange stresses.

Figure 5 — Comparison of stresses in boxes with varying taper. T = 100,000 inch-pounds.

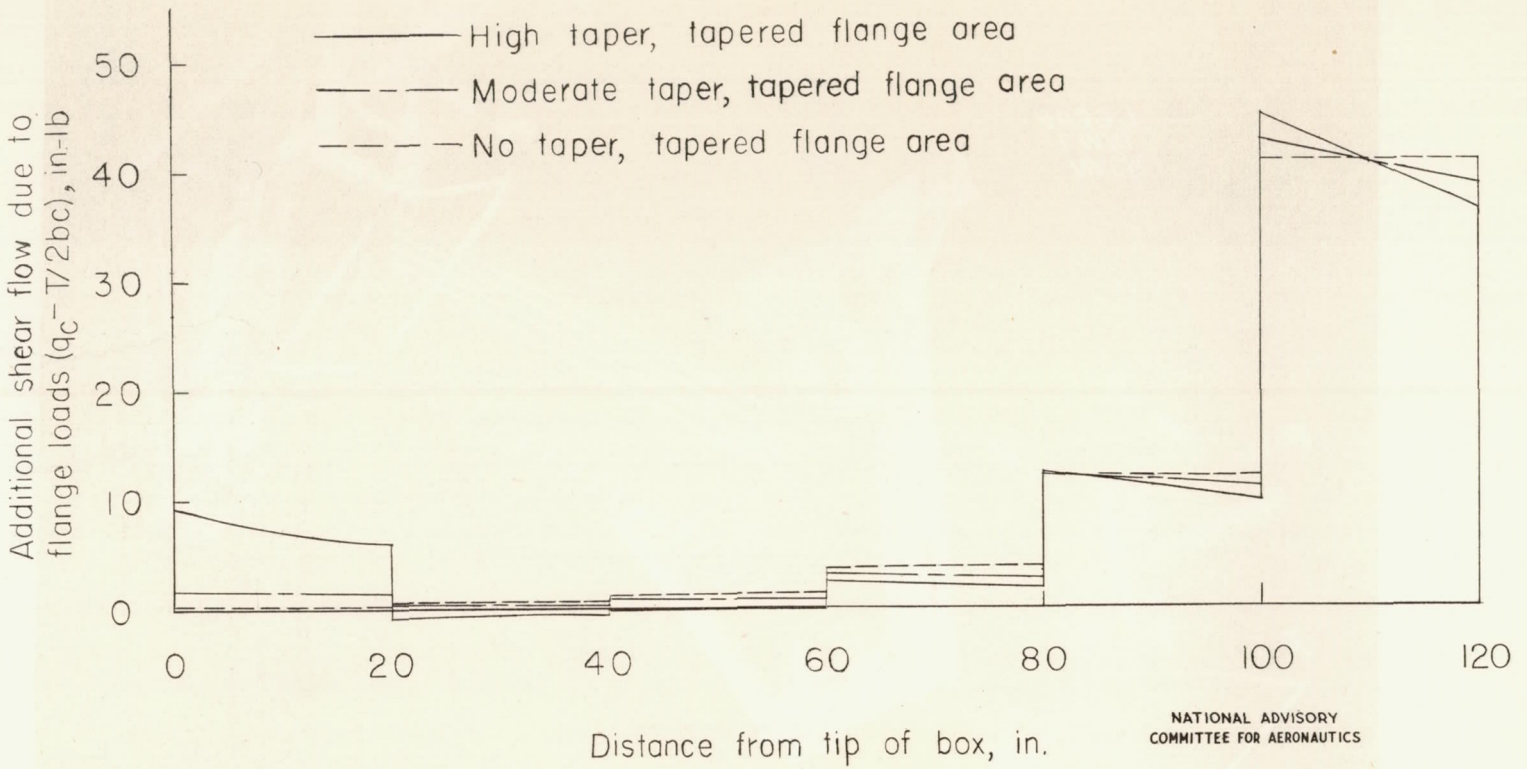

(b) Sheet stresses.

Figure 5.— Concluded.

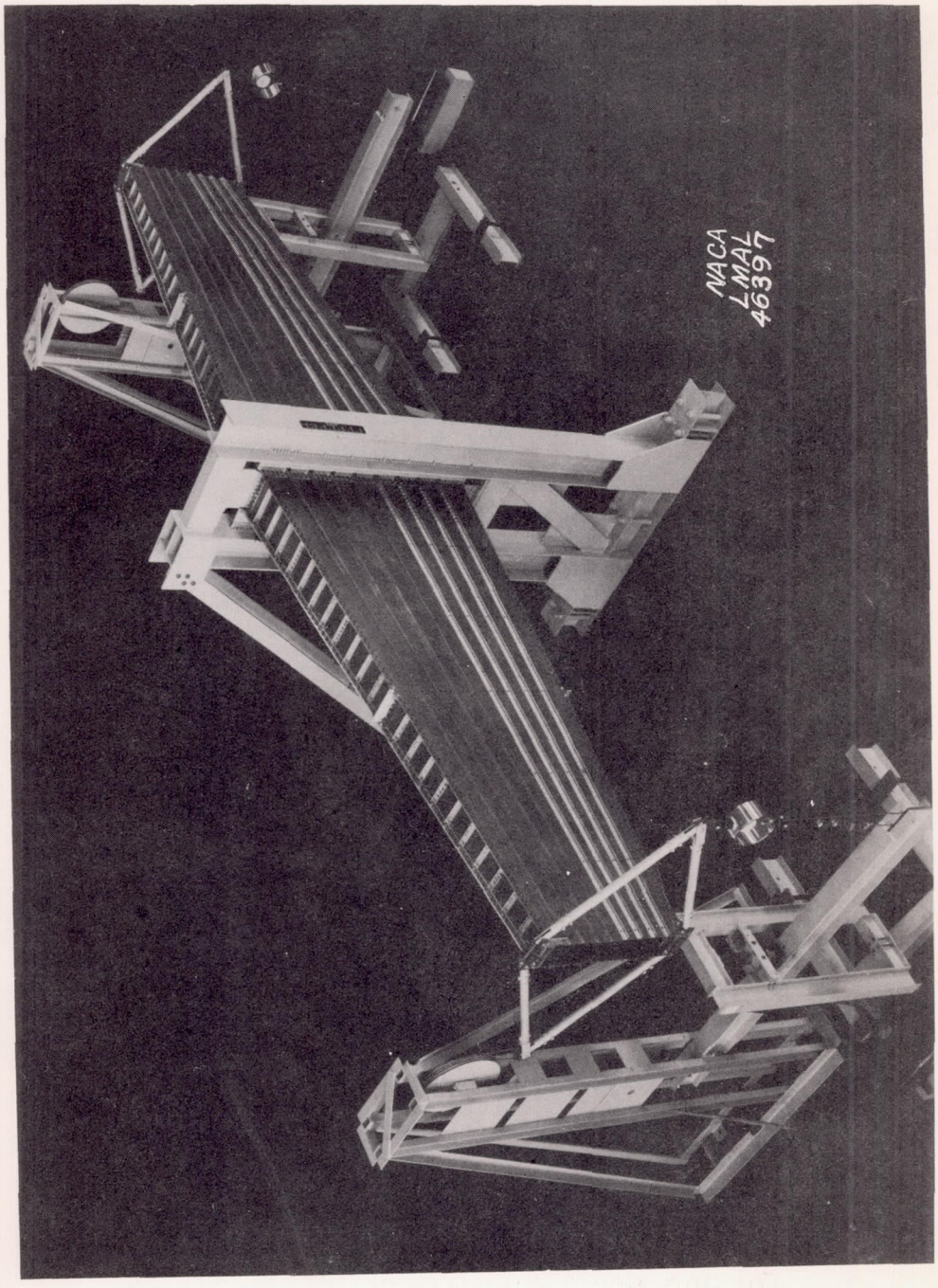

Figure 6.- Setup for torsion tests of tapered box beam.

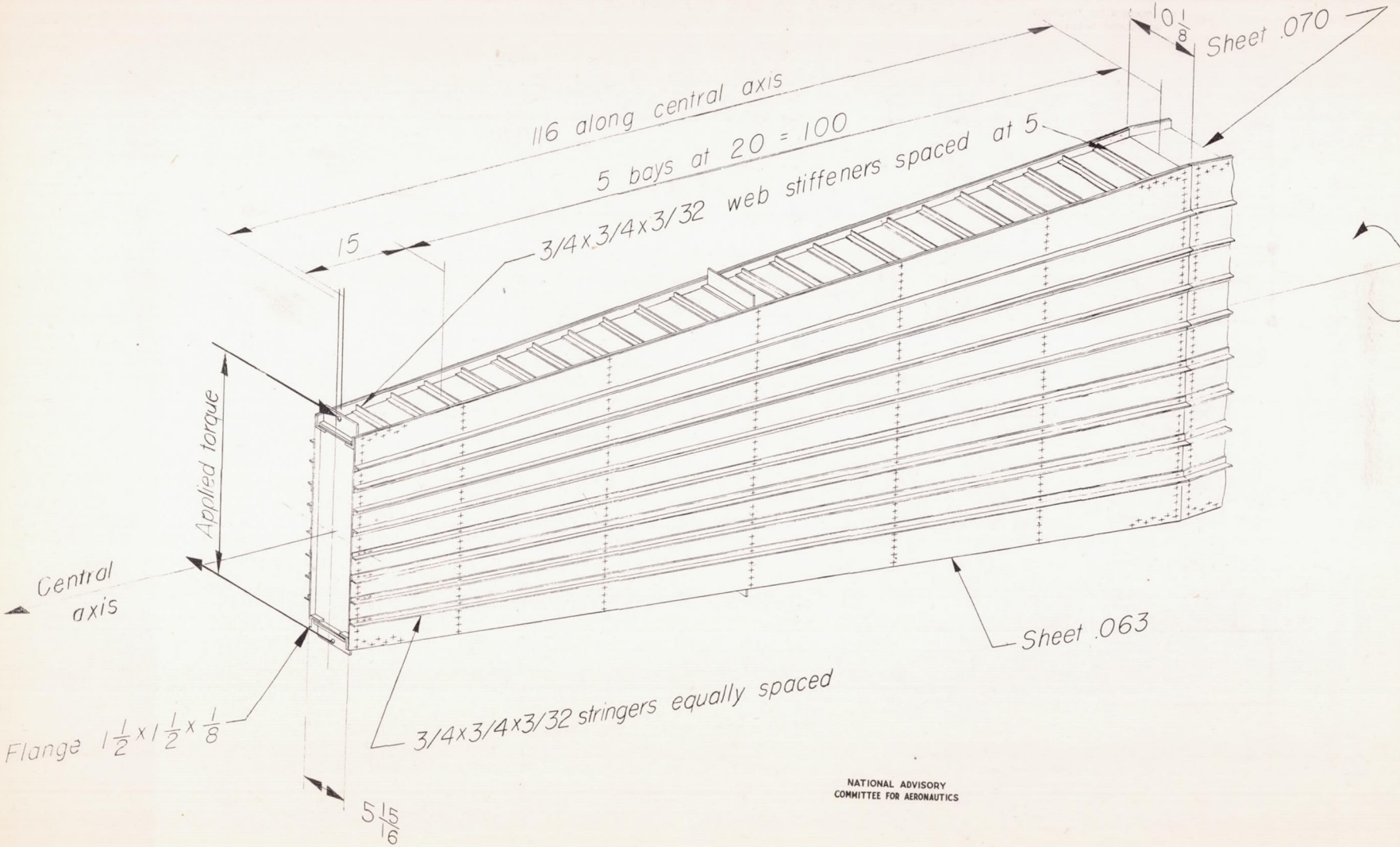

Figure 7.—Tapered box beam.

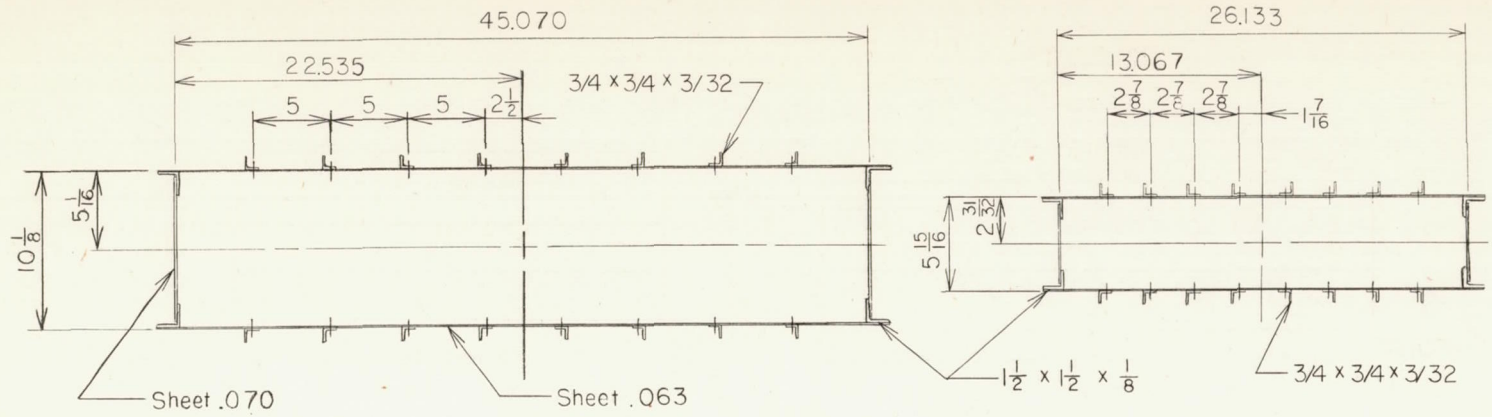

(a) Actual root and tip cross sections.

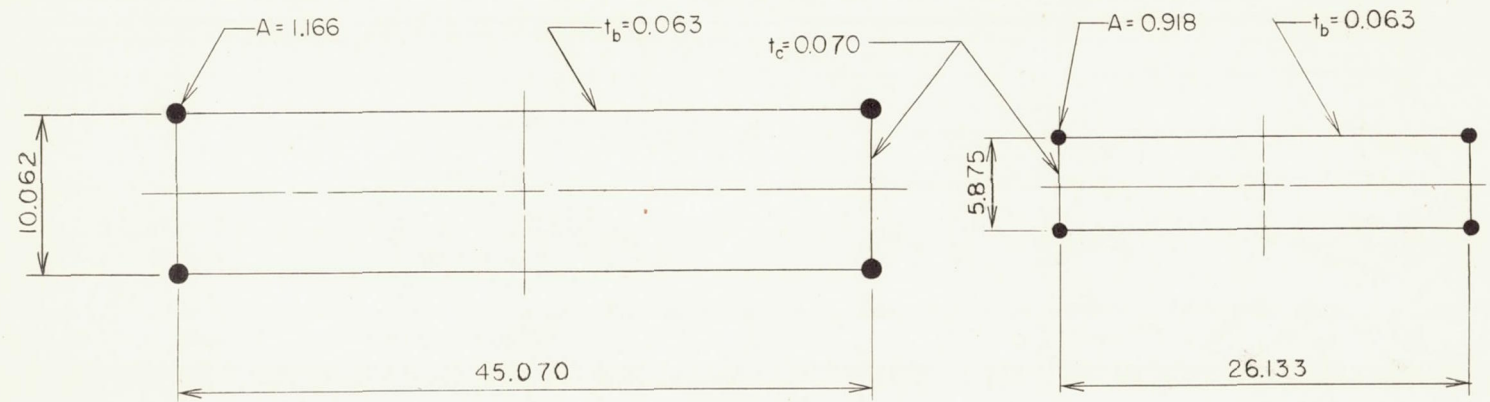

(b) Equivalent root and tip cross sections.

NATIONAL ADVISORY COMMITTEE FOR AERONAUTICS

Figure 8.—Actual and equivalent root and tip cross sections.

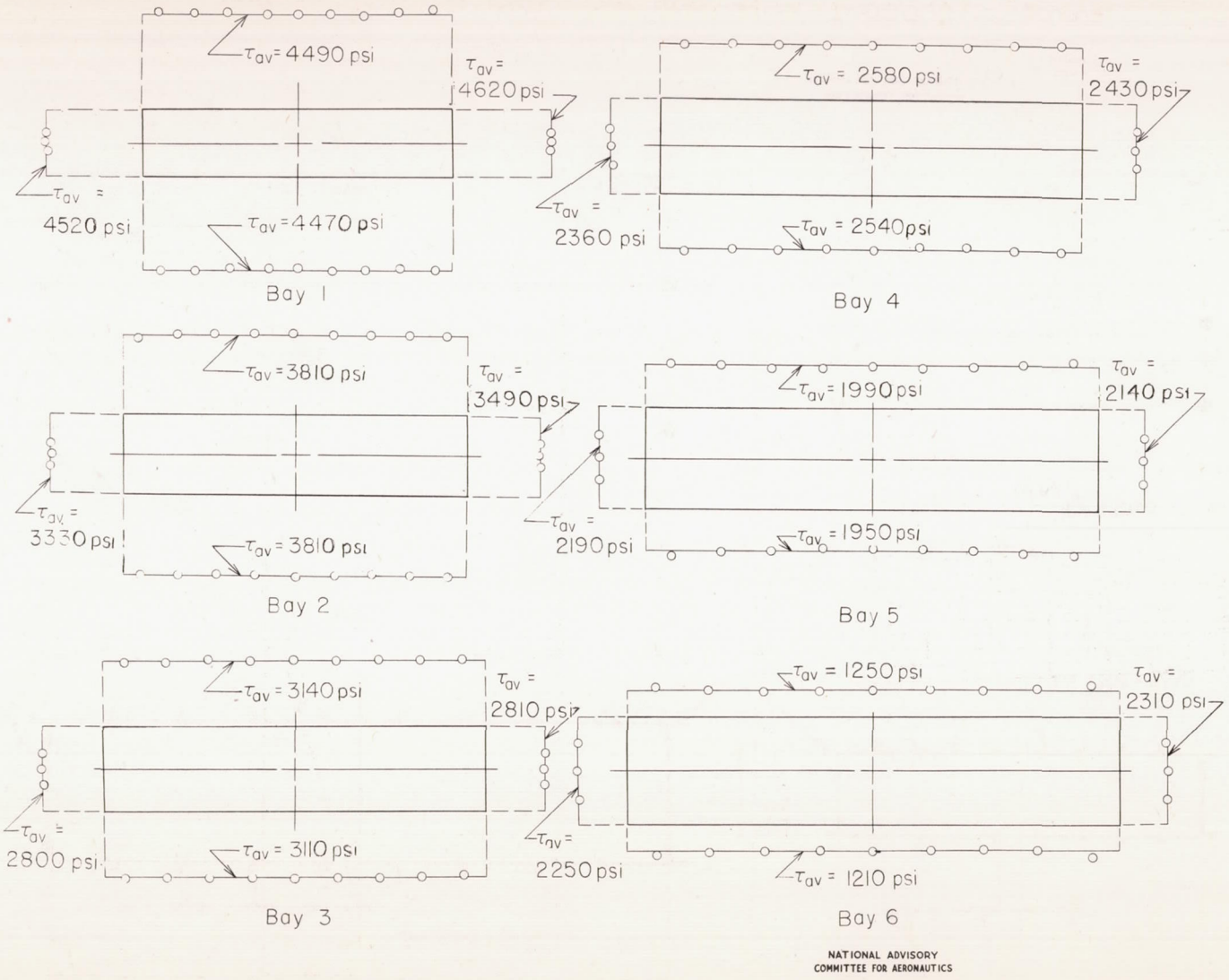

Figure 9—Distribution of shear stresses over cross section. T=100,000 inch-pounds.

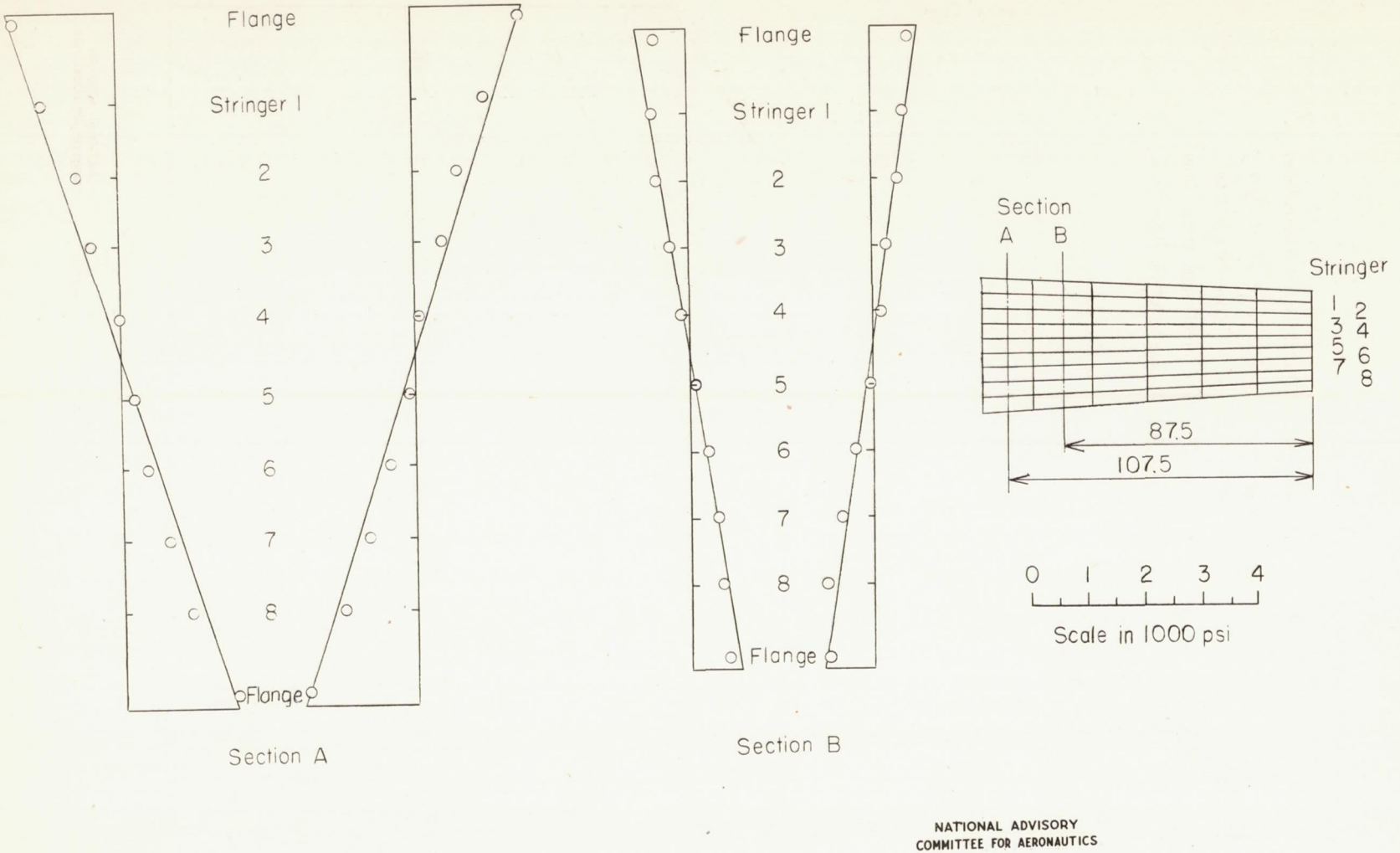

NATIONAL ADVISORY
COMMITTEE FOR AERONAUTICS

Figure 10.— Distribution of stringer stresses over cross section. T=100,000 inch-pounds.

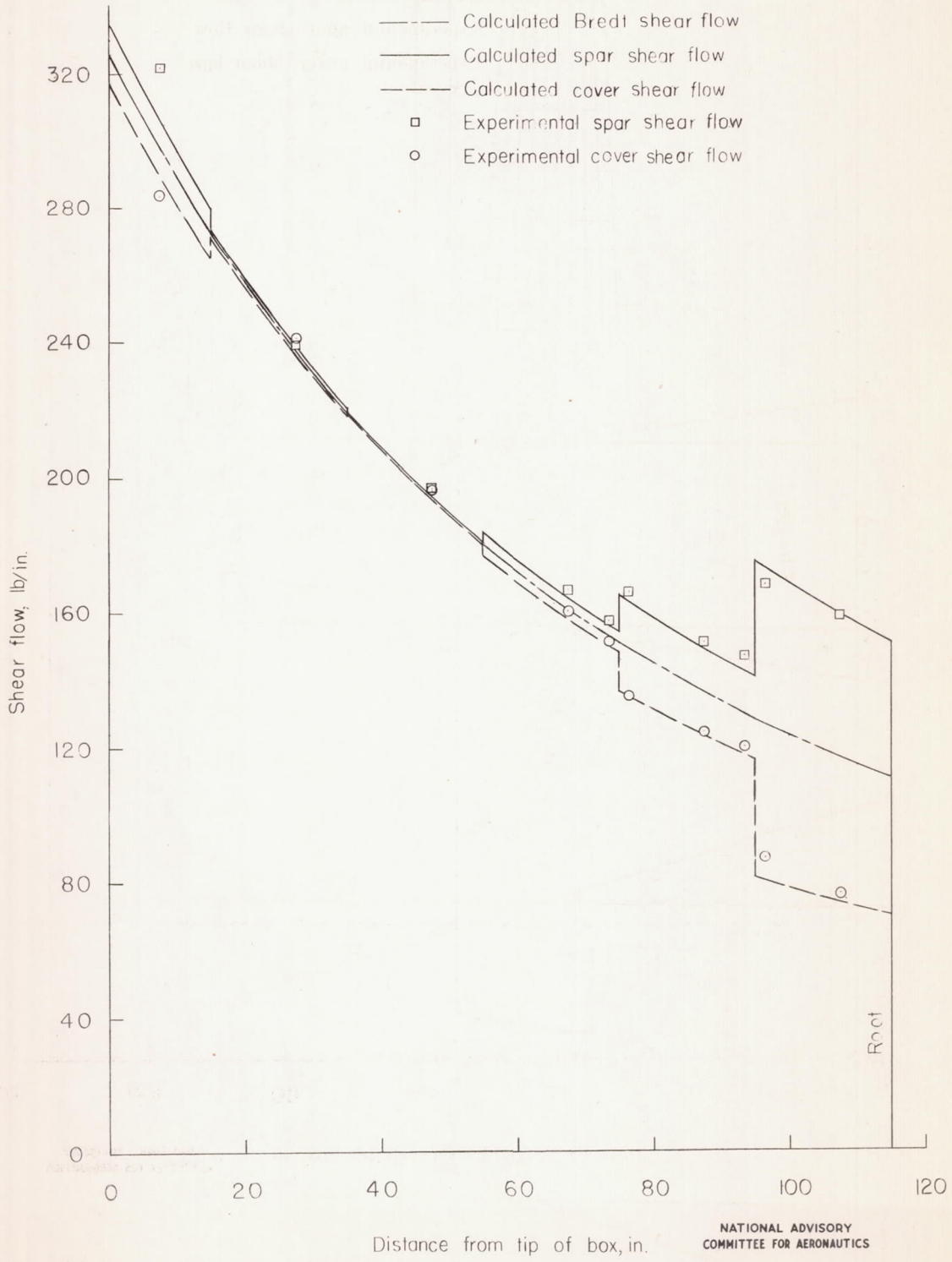

Figure 11.— Comparison of experimental and calculated shear flows for tip loading condition. T=100,000 inch-pounds.

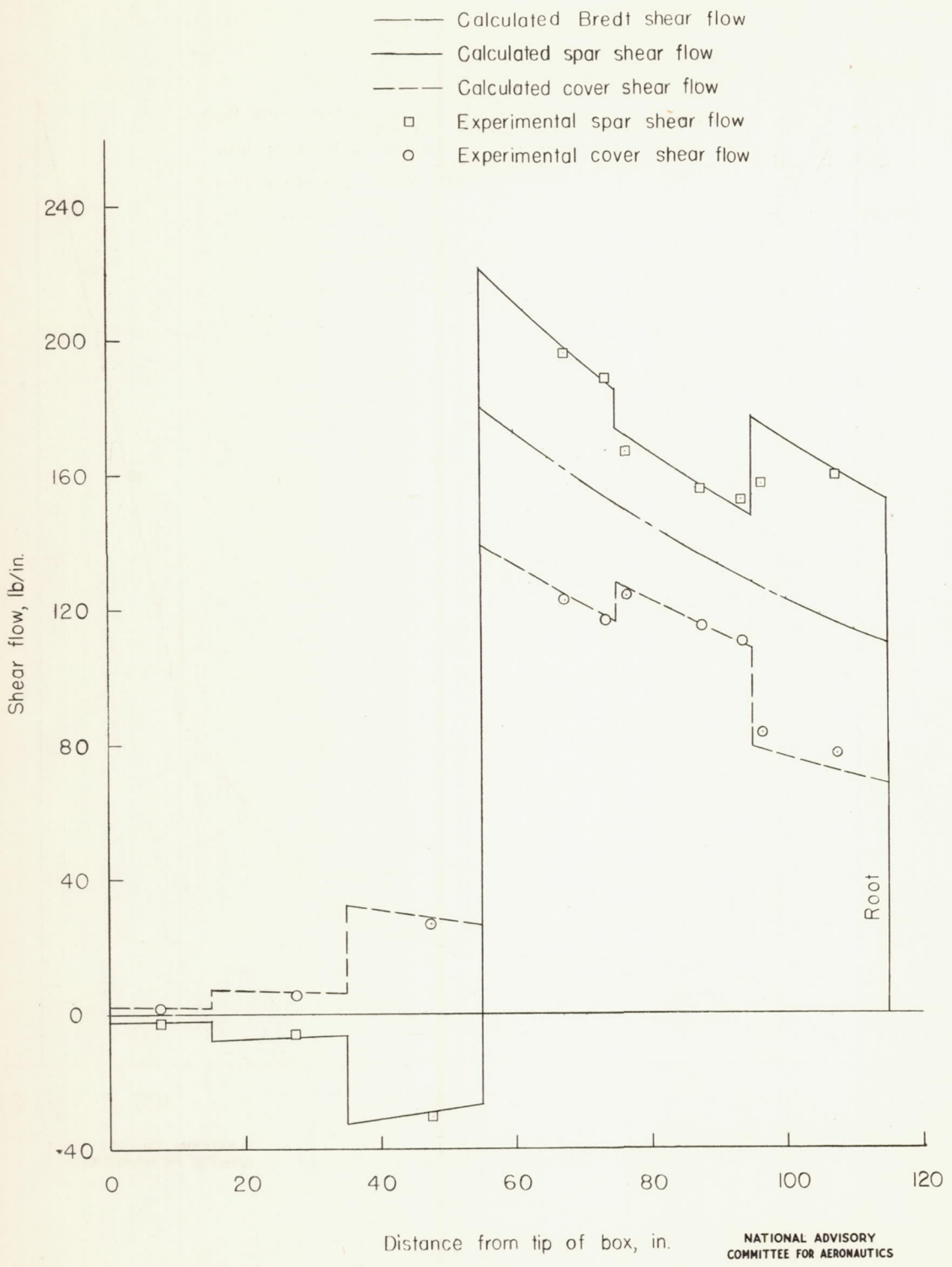

Figure 12.— Comparison of experimental and calculated shear flows for quarter-point loading condition. T = 100,000 inch-pounds.

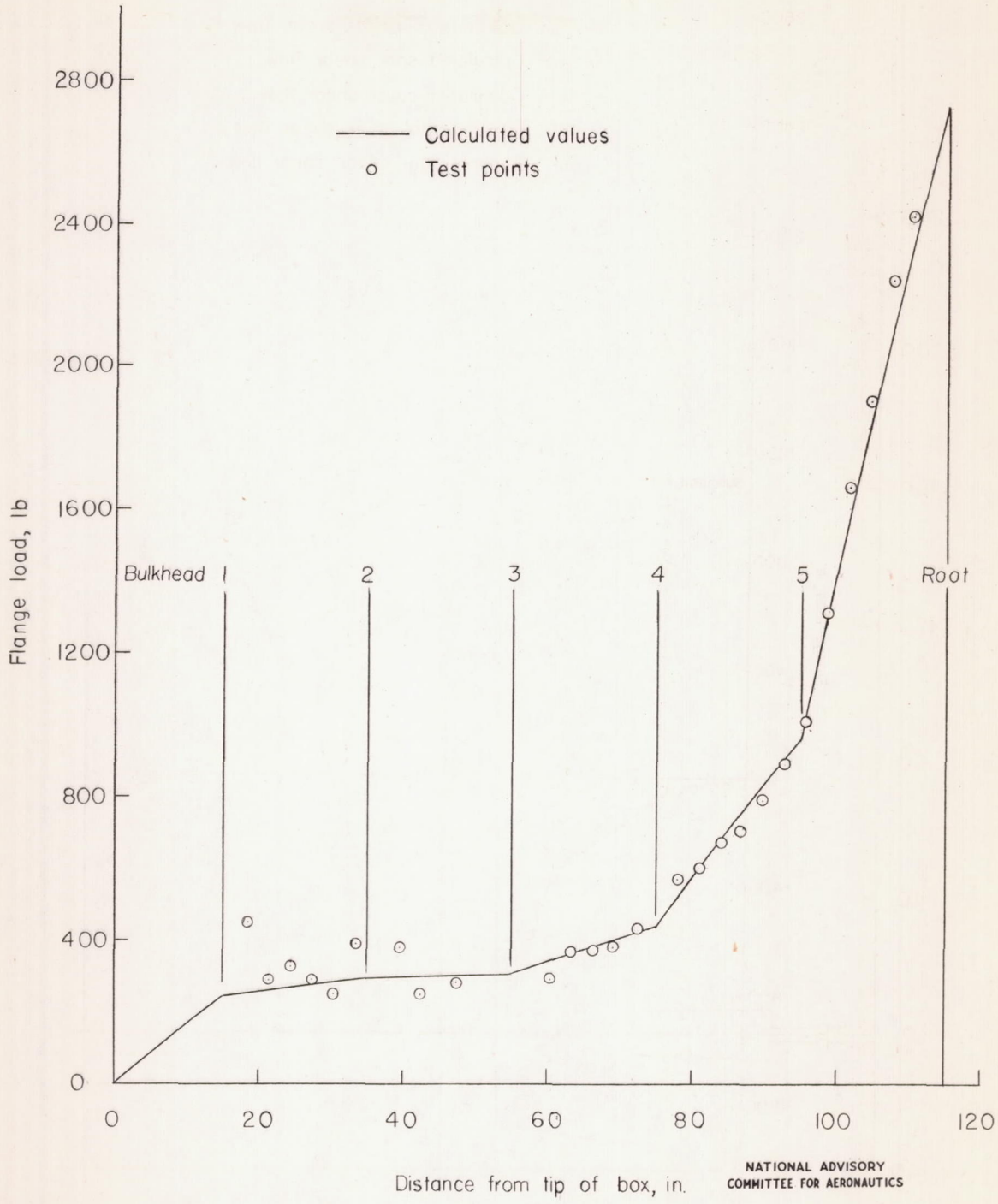

Figure 13.— Comparison of experimental and calculated flange loads for tip loading condition. T = 100,000 inch-pounds.

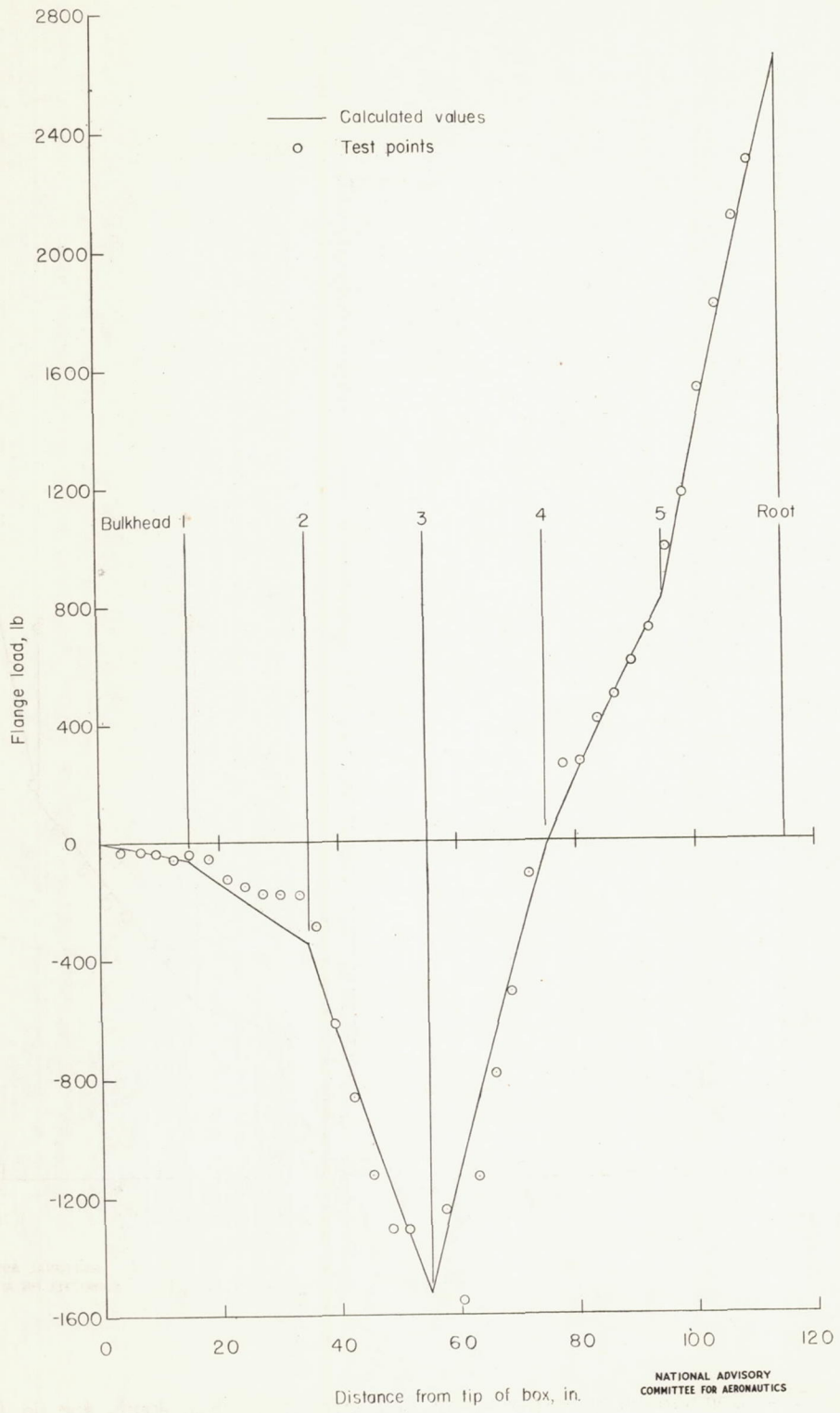

Figure 14.— Comparison of experimental and calculated flange loads for quarter-point loading condition, T=100,000 inch-pounds.